

# Preparation and Analysis of Cross-Linking Copolymers

Endre Szuromi, Márta Berka, and János Borbély\*

Department of Colloid Chemistry, Lajos Kossuth University, PO Box 31, H-4010 Debrecen 10, Hungary

Received June 2, 1999; Revised Manuscript Received November 15, 1999

**ABSTRACT:** Copolymerization of ST (styrene) with EDM (ethylene glycol dimethacrylate) gives nonlinear polymers. The average molecular weight and polydispersity of copolymers composed of ST and EDM were measured using the GPC (gel permeation chromatography) technique, and an exponential increase in both quantities with reaction time was observed.  $^1\text{H}$  and  $^{13}\text{C}$  NMR spectra of the copolymers were taken to prove the structure and purity of the products and to calculate the composition and pendant content of the copolymers. The ratio of the pendant double bonds of the copolymers was determined from the  $^1\text{H}$  NMR spectra. A remarkable increase in the ratio of the pendant double bonds with reaction time was observed. The mechanism for the chain propagation was studied and found to follow the terminal model. Reactivity ratios were found to be  $r_1 = 0.452 \pm 0.031$  for monomer ST and  $r_2 = 0.297 \pm 0.027$  for monomer EDM. According to the size distribution of the copolymers measured by DLS (dynamic light scattering) and the average radii of gyration measured by SLS (static light scattering) techniques, the samples showed strong polydispersity and an increase in molecular size with reaction time. Unusually high molecular weight values were observed after a certain reaction time.

## Introduction

The pathways for cross-linking copolymerization consist of solution and gel state reactions. In solution at low conversion the main process is the addition of monovinyl ( $M_1$ ) and divinyl ( $M_2$ ) monomers to linear radicals when the macroradicals formed contain reactive pendant double bonds. At higher conversion the addition of  $M_1$  and  $M_2$  to pendant double bonds may become significant. This step leads to the formation of side chains. Also at higher conversion the addition of macroradicals to pendant double bonds may occur. Along with these reactions of the pendant double bonds cyclization reactions take place. There are two types of cyclization reactions<sup>1–3</sup> in cross-linking copolymerization. The first type is called primary intramolecular cyclization reaction. In this case the pendant double bond reacts with the terminal radical of the same chain. The second type is the secondary intramolecular cyclization reaction. In this reaction the pendant double bond reacts with a radical on a side chain of the same molecule. The structures formed in intramolecular cyclization reactions are called microgels.<sup>2,4</sup> Cyclization happens predominantly in the early stage of the copolymerization, leading to decreased coil size at the same molecular weight.<sup>5</sup> The initiation of the pendant double bonds is also a solution state reaction of the pendant groups. When the polymer concentration becomes considerably higher, the formation of networks through cross-linkages is possible (see Figure 8). It occurs in the gel state.

The pathways for cross-linking copolymerization can be described more precisely with kinetic methods.<sup>6–13</sup> Studies dealing with the effect of the above-mentioned pathways on the average molecular weight are available.<sup>14</sup> It was proved that some of the pathways affect the average molecular weight. The addition of macroradicals to pendant double bonds causes a significant increase in  $\bar{M}_n$  and a smaller increase in  $\bar{M}_w$ . The cyclization reactions do not affect the average molecular

weight but cause a delay in gelation by consuming pendant double bonds. The initiation of the pendant double bonds has the same effect, but in addition it results in an increase in  $\bar{M}_n$  by decreasing the number of dead chains.

Both the pregelation<sup>15</sup> and the postgelation<sup>16,17</sup> periods were thoroughly studied by Okay et al.

In this study the solution polymerization of the monofunctional styrene (ST) and the bifunctional ethylene glycol dimethacrylate (EDM) was investigated. (Note: according to Flory's definition, these monomers are bi- and tetrafunctional, respectively.) The main properties investigated were molecular weight, monomer composition, and pendant content of the copolymers.

## Experimental Section

**Materials.** The solvent and the initiator used were toluene and azobis(isobutyronitrile) (AIBN), respectively. The stabilizers of the monomers being 4-*tert*-butylcatechol for ST and hydroquinone monomethyl ether for EDM were removed by extraction with 10% NaOH solution followed by extraction with distilled water, and the monomers were then distilled at low pressure. The initiator was recrystallized from methyl alcohol.

**Methods. (a) Solution Preparation.** Before the reactions the solutions with 1.39 M overall monomer concentration were taken under the freeze–thaw technique in 10 mL ampules. The ampules were then closed under vacuo. The reactions were carried out at 60 °C. Samples were taken in the pregelation period and then mixed with 10-fold excess methyl alcohol, and the copolymer precipitate was removed using an ultracentrifuge. The copolymers were then purified by dissolution in methylene chloride followed by precipitation with excess methyl alcohol. The samples were again centrifuged. This purification process was then repeated. This process was followed by drying at ambient temperature.

**(b) Analysis.** GPC measurements were carried out using a Waters instrument. Calibration was done with polystyrene standards with peak molecular weights ( $M_p$ ) in the range 580–2 750 000 g/mol in solution with THF (tetrahydrofuran;  $c = 0.5\%$  m/m). Only molecular weights falling in this region could be measured.

NMR measurements were taken on a Bruker 200 SY NMR instrument to elucidate the structure of the macromolecules.

\* To whom correspondence should be addressed.

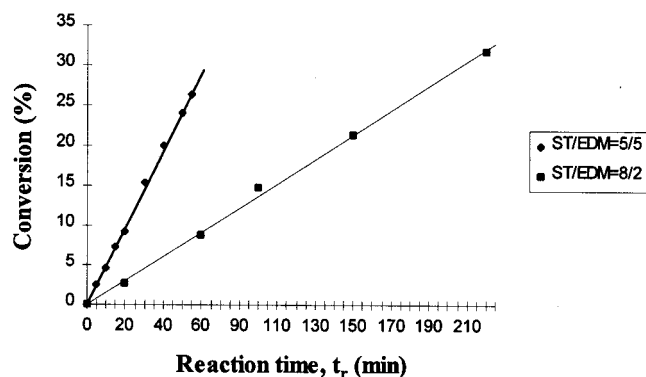


**Figure 1.** Conversion–reaction time curves for ST-EDM copolymers (ST/EDM = 5/5 and 8/2).

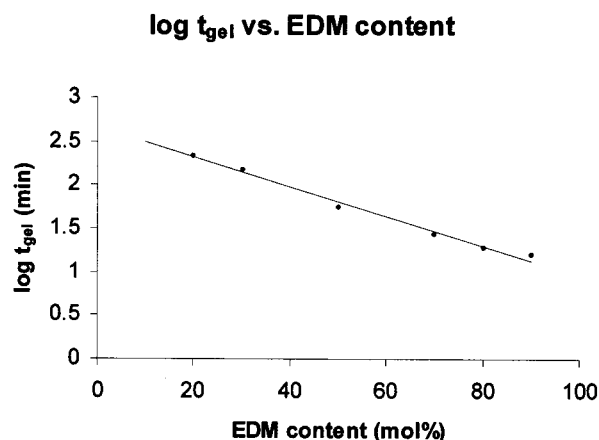


**Figure 2.** Effect of monomer composition on gelation time for ST-EDM copolymers.

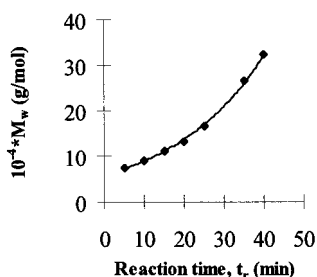


**Figure 3.**  $\bar{M}_w$ –reaction time curve for ST-EDM copolymers (ST/EDM = 5/5).

Solvents were  $\text{CDCl}_3$  (99.8 at. % D) and  $(\text{CD}_3)_2\text{CO}$  (99.8 at. % D) depending on the solubility of the samples ( $c = 2.0$  mg/mL).  $\text{CDCl}_3$  was found to dissolve the samples better than  $(\text{CD}_3)_2\text{CO}$ , but the quantitative analysis of the NMR spectra of the samples dissolved in  $(\text{CD}_3)_2\text{CO}$  was easier since no solvent peaks appeared in the region used for the calculations. In the case of the NMR spectra of the samples dissolved in  $\text{CDCl}_3$  the integral value of the residual  $\text{CHCl}_3$  peak at 7.26 ppm had to be subtracted from that of the wide peak of the styrene unit of the copolymer.

The SLS and DLS measurements were carried out by a Brookhaven Laser Light Scattering Research System at  $\lambda = 532$  nm. SLS measurements were typically made as a function of both scattering angle ( $\theta = 30^\circ$ – $142.5^\circ$ ) and macromolecular concentration ( $c = 0.01$ – $0.4$  mg/ $\text{cm}^3$ ) in THF solution (similar to GPC measurements). The specific refractive index increment of the solution was measured by an interferometer ( $dn/dc = 0.08$ – $0.18$   $\text{cm}^3/\text{g}$ ); the molecular weight and radius of gyration<sup>18</sup> were determined by fitting to Zimm plots. In the application of DLS for particle sizing and size distribution the autocorrelation functions were also obtained at different angles ( $\theta =$

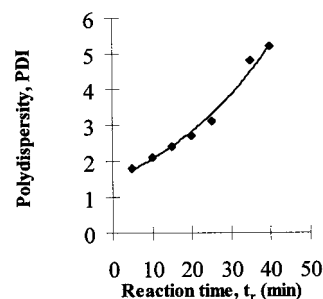


**Figure 4.** Polydispersity–reaction time curve for ST-EDM copolymers (ST/EDM = 5/5).

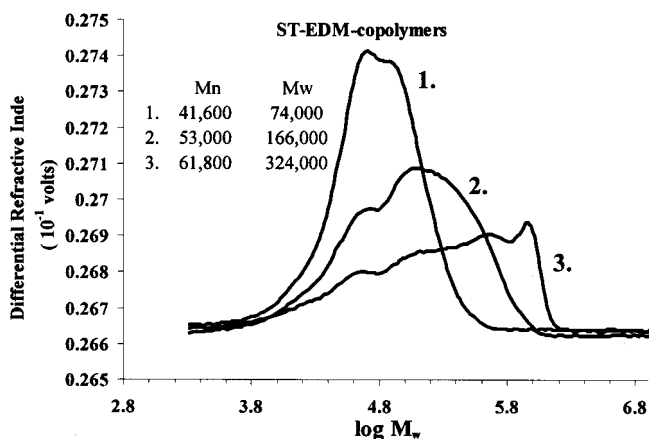


**Figure 5.** GPC curves for ST-EDM copolymers (ST/EDM = 5/5, reaction time = 1 min (1), 25 min (2), and 40 min (3)).

**Table 1. Changes of Particle Size and Polydispersity with Reaction Time for ST-EDM Copolymers (ST/EDM = 5/5, Reaction Time = 5, 25, and 35 min)**

reaction time (min)	5	25	35
radius of gyration (nm)	$20 \pm 0.5$	$40 \pm 1$	$60 \pm 2$
by SLS			
$\bar{M}_w$ by GPC	87600	227500	390300
PDI <sup>a</sup> by GPC	1.9	4.0	5.6

<sup>a</sup> PDI has only qualitative meaning in the case of multimodal peaks (see Figure 7).

$30^\circ$ – $142.5^\circ$ ). The stock solutions were cleaned by  $1 \mu\text{m}$  pore-size filters. The concentration of the solutions was remeasured after filtration.

## Results and Discussion

**Conversion.** The conversion–reaction time function was found to be linear and crossing the  $y$ -axis at zero conversion. This proves that inhibition did not take place. Figure 1 shows the results for a system with monomer ratios ST/EDM = 5/5 and 8/2 in the feed. The two curves have different slopes which shows that the reaction with ST/EDM = 5/5 monomer composition is significantly faster than with the monomer composition ST/EDM = 8/2. It can be explained via kinetic methods which is out of the scope of this paper. The conversion was monitored up to the gelation point. To stop the reaction before gelation, we had to determine the gelation point. It was determined by visual observation. We used this method for ST/EDM systems with different monomer ratio. A more precise determination of the gelation point was not necessary as our work was focused only on the pregelation period. Gelation time was found to be changing logarithmically with the monomer composition as shown in Figure 2.

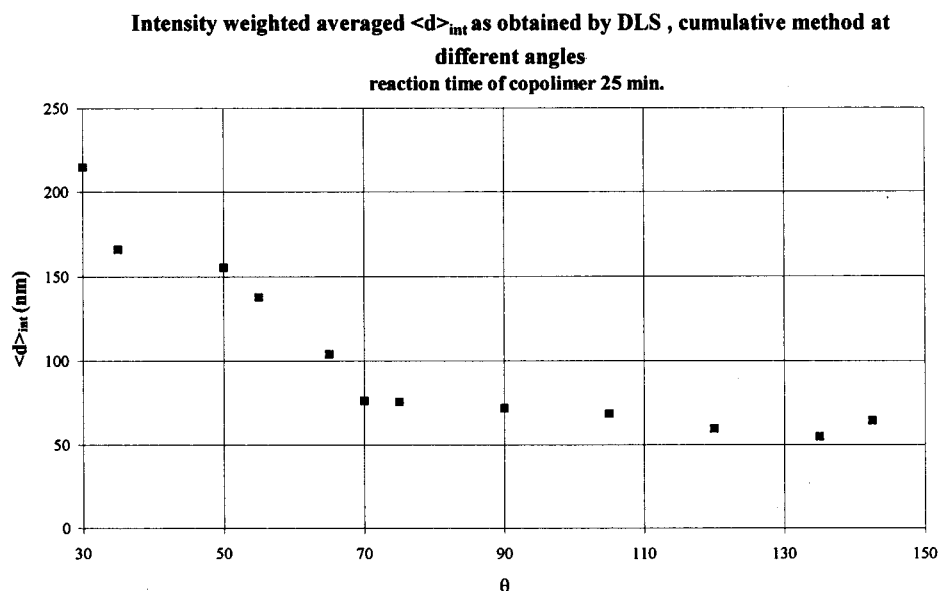


**Figure 6.** DLS measurement results (ST/EDM = 5/5, reaction time = 25 min).

**Molecular Weight and Polydispersity.** Both molecular weight ( $M_w$ ) and polydispersity (PDI) showed an exponential increase with reaction time. In Figure 3 and Figure 4 these changes can be seen for a system with the monomer ratio ST/EDM = 5/5 in the feed. Calculating a single value of PDI is not valid for multimodal systems; therefore, it should be noted that the curve shown in Figure 4 has only qualitative importance in the longer reaction time region as in this region samples give multimodal GPC curves.

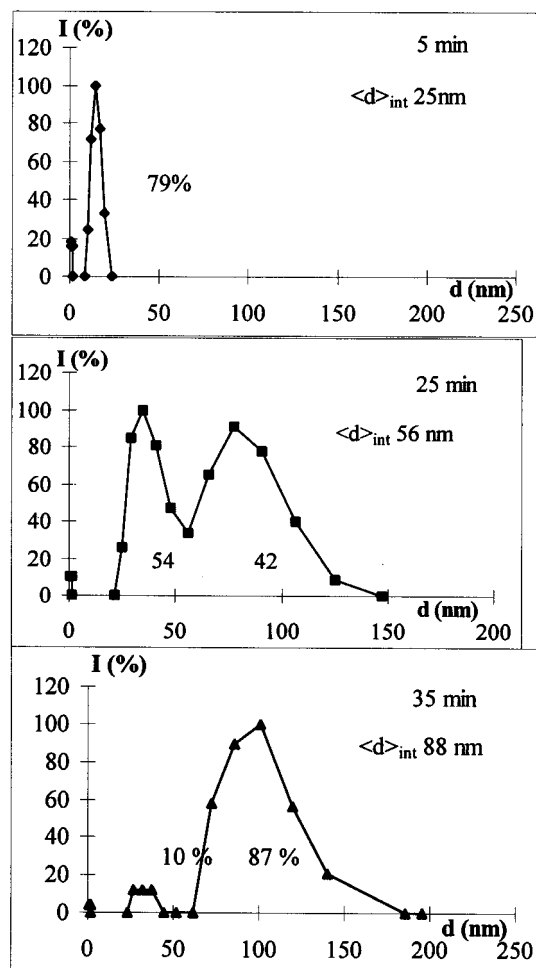
Figure 5 gives an informative view of the process. (Note that for sample 3 the exclusion limit of the GPC setup is approached.) The increase in the width of the curves means that the polydispersity gets higher as the reaction progresses, and it can also be seen from the shift to the right that larger molecules form as the reaction time increases. This might be the result of the addition of macroradicals to pendant double bonds. Mainly this reaction is responsible for the average molecular weight change in solution state.

**Laser Light Scattering Results.** The average radii of gyration measured by the SLS technique as a function of reaction time are shown in Table 1 (ST/EDM = 5/5, reaction time = 5, 25, and 35 min).

The average radius of gyration for the copolymers measured by the SLS technique significantly increases with the reaction time. To obtain more information about polydispersity, the samples were examined by DLS at different angles. Calculated with the cumulative method, the polydispersity index (defined as  $K_2/I$ ) is high enough at every angle, and the experimentally determined  $\theta$  dependence of the intensity mean diameter ( $\langle d \rangle_{\text{int}}$ ) also shows strong polydispersity of the samples. Figure 6 shows the intensity-weighted averaged effective diameter obtained by DLS. The advantage of the DLS method is that the size of those large molecules that cannot be measured with GPC (see Figure 5) can be measured.

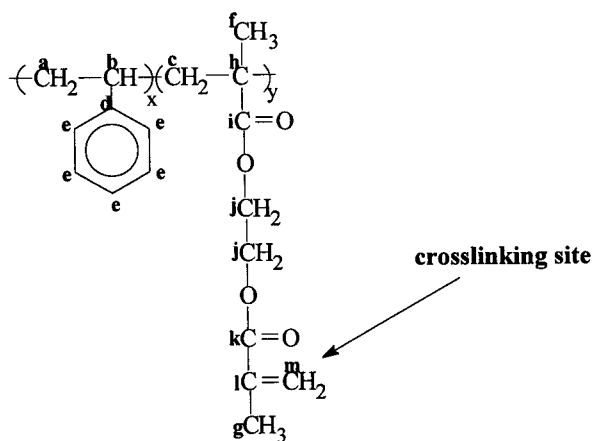
At the angle  $\theta = 90^\circ$  the effect of impurities is negligible; therefore, the polydispersity only reflects that of the sample.

Figure 7 shows the size distributions calculated by NNLS. The average values increase, and the distribu-



**Figure 7.** Intensity-size distributions obtained by DLS at  $\theta = 90^\circ$ ,  $\lambda = 532$  nm, calculated by NNLS (ST/EDM = 5/5, reaction time = 5, 25, and 35 min).

tion curve shifts toward the high molecular size region; the ratio of the large particles increases. The intensity of the large particles gives an increasing part of the sum intensity. However, while the size distribution obtained



**Figure 8.** Schematic structure of ST-EDM copolymers.

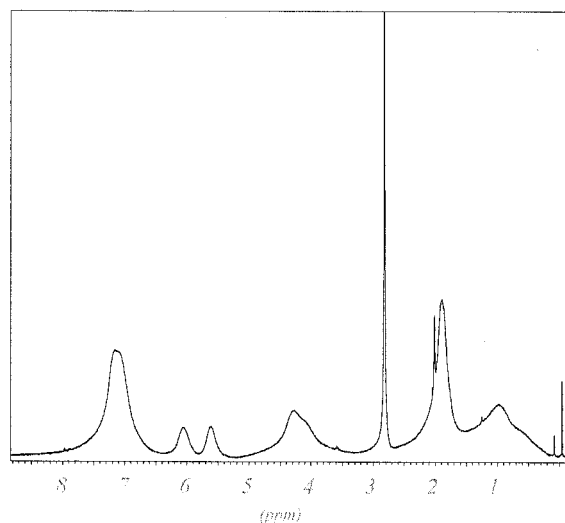


**Figure 9.**  $^1\text{H}$  NMR spectrum of a ST-EDM copolymer sample in acetone- $d_6$  (ST/EDM = 5/5, reaction time = 15 min, conversion = 3.4%).

in a DLS experiment is weighted by the ability of the particles to scatter, it is impossible to obtain a quantitative characterization of the exact shape of the size or molar mass distribution. The attempts to convert the intensity-weighted size distribution to size distribution may result in rather large errors. The original intensity-weighted size distribution has much important information, and it is able to detect very small amounts of large particles.

**Structure and Composition.** The schematic structure of the copolymer prepared is shown in Figure 8.

The structural units of the copolymers could easily be identified from the  $^1\text{H}$  and  $^{13}\text{C}$  NMR spectra. The samples were dissolved in acetone- $d_6$  or chloroform- $d$  ( $c = 2.0\%$  m/m for  $^1\text{H}$  NMR and  $10.0\%$  m/m for  $^{13}\text{C}$  NMR measurements). Mainly the  $^1\text{H}$  NMR technique was used to analyze the samples both qualitatively and quantitatively, but  $^{13}\text{C}$  NMR measurements were also taken not only to confirm the  $^1\text{H}$  NMR data interpretation but also to give more details on the actual structure of the products. There are some structural units that cannot be measured with  $^1\text{H}$  NMR (e.g., carbonyl group) or overlap too much in the  $^1\text{H}$  NMR spectrum (e.g., alkyl groups). These structural units can be perfectly assigned by the  $^{13}\text{C}$  NMR technique. Figure 9 shows the  $^1\text{H}$  NMR spectrum of the purified copolymer formed in a reaction mixture with the monomer ratio ST/EDM = 5/5 after

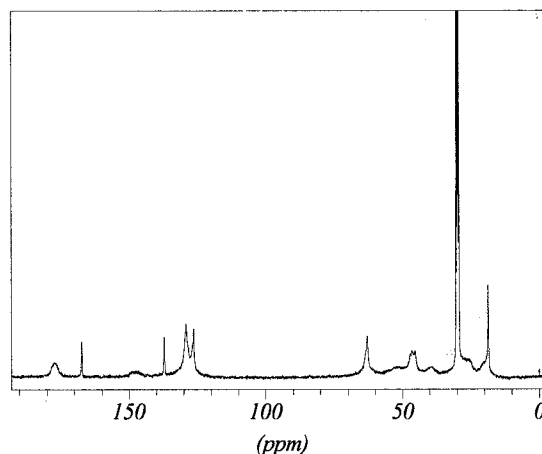


**Figure 10.**  $^{13}\text{C}$  NMR spectrum of a ST-EDM copolymer sample in acetone- $d_6$  (ST/EDM = 5/5, reaction time = 15 min, conversion = 3.4%).

**Table 2.**  $^1\text{H}$  NMR Peak Assignment of an ST-EDM Copolymer (ST/EDM = 5/5, Reaction Time = 15 min, Conversion = 3.4%)

chemical shift (ppm)	corresponding structural unit	chemical shift (ppm)	corresponding structural unit
0.1–2.3	a, b, c, f, g	5.9–6.3	m
3.6–4.6	j	6.7–7.5	e
5.4–5.7	m		

**Table 3.**  $^{13}\text{C}$  NMR Peak Assignment of an ST-EDM Copolymer (ST/EDM = 5/5, Reaction Time = 15 min, Conversion = 3.4%)

chemical shift (ppm)	corresponding structural unit	chemical shift (ppm)	corresponding structural unit
19	f, g	136	l
32–57	a, b, c, h	140–152	d
60–64	j	167	k
125	m	174–179	i
127–130	e		

**Table 4.** Composition of ST-EDM Copolymers Depending on the Composition of the Reaction Mixtures

EDM molar ratio in the feed ( $m_2$ )	EDM molar ratio in the copolymer ( $p_2$ )	EDM molar ratio in the feed ( $m_2$ )	EDM molar ratio in the copolymer ( $p_2$ )
0.1000	0.1720	0.6000	0.5260
0.2000	0.2700	0.7000	0.5920
0.3000	0.3580	0.8000	0.6740
0.4000	0.4190	0.9000	0.7660
0.5000	0.4650		

15 min reaction time dissolved in acetone- $d_6$ . The chemical shift values and the corresponding structural units are listed in Table 2. For labels see Figure 8.

Figure 10 shows the  $^{13}\text{C}$  NMR spectrum of the same sample also dissolved in acetone- $d_6$ . The chemical shift values and the corresponding structural units are listed in Table 3. For labels see Figure 8.

Using the  $^1\text{H}$  NMR spectra of the pure samples, it was possible to determine the composition of the copolymers. The integral values of the aromatic hydrogens in ST between 6.7 and 7.5 ppm and of the  $-(\text{CH}_2)_2-$  unit in EDM between 3.6 and 4.6 ppm were compared in the calculation of the composition of the copolymer. The results are shown in Table 4.

The data in Table 4 were calculated for reactions with conversions no higher than 10%, because only in this case is the Kelen–Tüdös (KT) equation<sup>19</sup> valid for the calculation of the reactivity ratios of the monomers. The



Table 5. Dependence of the Pendant Ratio of ST-EDM Copolymers

$n_{ST}/n_{EDM}$ in feed	1/9	2/8	3/7	4/6	5/5	25	35	55	6/4	7/3	8/2	9/1
reaction time, $t_r$ (min)	5	3	10	20	5	5.7	10.1	14.3	5.6	5.3	5.3	5.3
conversion (%)	2.4	0.7	3.1	7.8	1.2	66.2	69.2	81.1	75.1	62.0	54.5	43.7
pendant concn in polymer (%)	87.8	73.5	79.6	81.2	59.2							

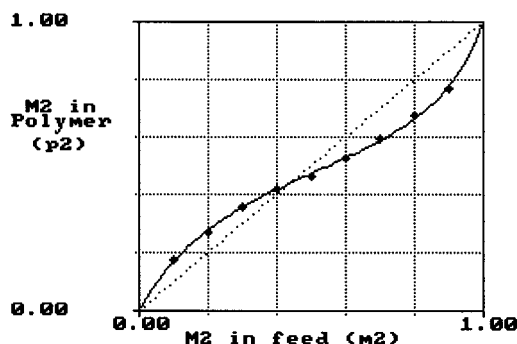
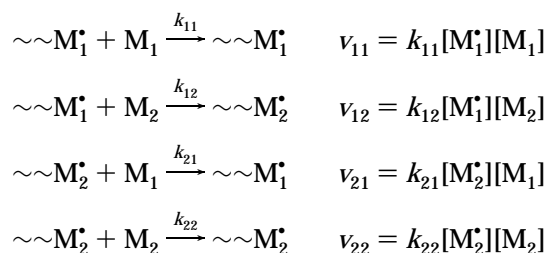


Figure 11. Copolymerization composition diagram for ST-EDM copolymers.

meaning of the reactivity ratios is easily understood from the following scheme. The chain propagation consists of the following steps:



The reactivity ratios are  $r_1 = k_{11}/k_{12}$  for ST and  $r_2 = k_{22}/k_{21}$  for EDM. These reactivity ratios for our reaction were found to be  $r_1 = 0.452 \pm 0.031$  and  $r_2 = 0.297 \pm 0.027$ . In the literature one can find numerous data on the copolymerization parameters of ST with different monomers containing one vinyl group.<sup>20,21</sup> Our result gives well-calculated data for a divinyl-containing system which is very much unique.

Using the  $r_1$  and  $r_2$  values, it was possible to construct the composition diagram (see Figure 11), which is a very important result, since it gives a relation between the composition of the reaction mixture and the composition of the copolymer formed in that specific reaction mixture. This way it is possible to control the composition of ST/EDM copolymers.

**Pendant Double Bonds.** The integral values of the corresponding peaks in the  $^1\text{H}$  NMR spectra, namely those of the vinyl hydrogens between 5.4 and 5.7 ppm and 5.9 and 6.3 ppm and the  $-(\text{CH}_2)_2-$  unit in EDM between 3.6 and 4.6 ppm, were used to calculate the ratio of the pendant double bonds of the copolymers. It was found that increasing the reaction time results in a significant increase in the ratio of the pendant double bonds of the copolymers (see Table 5, Figure 12). The process was thoroughly investigated with DSC<sup>22</sup> (differential scanning calorimetry), and the same tendency was found for this system. This might be explained by the fact that at lower conversion intramolecular cyclization reactions consume most of the double bonds, but at higher conversion since the size of the molecules increases as large macroradicals may form, side chains reacting with some of the pendant double bonds on the surface of the microgel cyclization reactions become

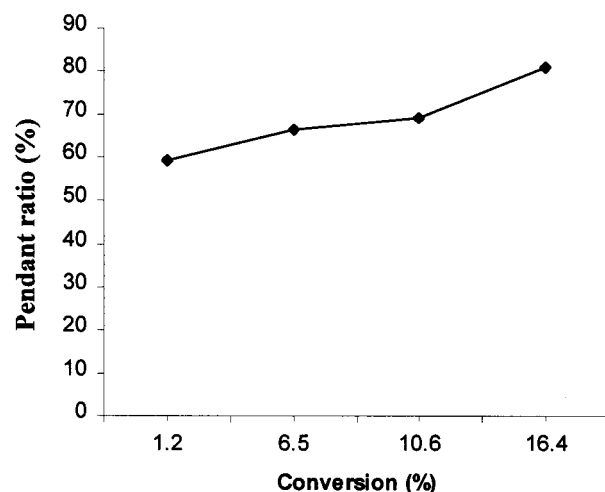


Figure 12. Dependence of the pendant ratio on the conversion (ST/EDM = 5/5, reaction time = 5, 25, 35, and 55 min).

sterically hindered. This results in the increase of the pendant double bonds. The concentration of the unreacted double bonds of the copolymers given as  $[\text{C}=\text{C}]/[\text{EDM}]$  increased with increasing EDM ratio in the reaction mixture. This tendency is shown in Table 5. The same results were gained by authors who applied Raman spectroscopy to monitor the system.<sup>23</sup>

**Conclusions.** Styrene-ethylene glycol dimethacrylate copolymers were prepared by free-radical polymerization reaction. The samples were analyzed with GPC, LS, and NMR instruments. The GPC and LS analyses gave consistent results on the molecular weight and molecular weight distribution changes in the system. We found that an exponential increase in both quantities occurs with increasing reaction time. The structural analyses ( $^1\text{H}$  and  $^{13}\text{C}$  NMR) showed that the construction of a composition diagram by the KT method for the monovinyl systems is possible for our system as well. We found that the ST/EDM system follows the terminal model. The measurement of the pendant double bonds gave a reactive group concentration increase with conversion. In conclusion, the ST/EDM system was found to follow the general paths for monovinyl-divinyl copolymerization given in the Introduction.

**Acknowledgment.** Financial support by the Hungarian Ministry of Culture and Education (Projects MKM FKFP 0444/1997, 0500/1997, and PFP 4276/1997), the Hungarian Scientific Research Fund (OTKA; Project number T 030025), and the US-Hungarian Science and Technology Joint Fund (JFN 355) is gratefully acknowledged.

## References and Notes

- (1) Dušek, K.; Ilavský, M. *J. Polym. Sci. Symp. Ser.* **1975**, *53*, 57, 75.
- (2) Dušek, K.; Galina, H.; Mikes, J. *Polym. Bull.* **1980**, *3*, 19.
- (3) Tobita, H.; Hamielec, A. E. *Polymer* **1990**, *31*, 1546.
- (4) Graham, N. B. *Makromol Chem., Macromol Symp.* **1995**, *93*, 293.

- (5) Dušek, K. In *Developments in Polymerization-3*; Appl. Sci.: London, 1982; Chapter 4.
- (6) Tobita, H.; Hamielec, A. E. *Macromol. Chem., Macromol. Symp.* **1988**, 20/21, 501.
- (7) Macosko, C. W.; Miller, D. R. *Macromolecules* **1976**, 9, 199.
- (8) Williams, R. J. J.; Vallo, C. I. *Macromolecules* **1988**, 21, 2568.
- (9) Dotson, N. A.; Galvan, R.; Macosko, C. W. *Macromolecules* **1988**, 21, 2571.
- (10) Anseth, K. S.; Rothenberg, M. D.; Bowman, C. N. *Macromolecules* **1994**, 27, 2890.
- (11) Kannurpatti, A. R.; Anderson, K. J.; Anseth, J. W.; Bowman, C. N. *J. Polym. Sci., Polym. Phys. Ed.* **1997**, 35, 2297.
- (12) Kannurpatti, A. R.; Bowman, C. N. *Macromolecules* **1998**, 31, 3311.
- (13) Matsumoto, A. *Adv. Polym. Sci.* **1995**, 123, 41.
- (14) Xie, T.; Hamielec, A. E. *Makromol. Chem., Theory Simul.* **1993**, 2, 777.
- (15) Okay, O.; Naghash, H. J.; Capek, I. *Polymer* **1995**, 36, 2413.
- (16) Okay, O. *Polymer* **1994**, 35, 796.
- (17) Okay, O. *Polymer* **1994**, 35, 2613.
- (18) Benoit, H.; Froehlich, D. *Light Scattering From Polymer Solutions*; Huglin, M. B., Ed.; Academic Press: New York, 1977; Chapter 11, p 467.
- (19) Kelen, T.; Tüdös, F. *J. Macromol. Sci., Chem.* **1975**, A-9, 1.
- (20) Braun, D.; Czerwinski, W.; Disselhoff, G.; Tüdös, F.; Kelen, T.; Turcsányi, B. *Angew. Makromol. Chem.* **1984**, 125, 161.
- (21) Braun, D.; Czerwinski, W.; Tüdös, F.; Kelen, T.; Turcsányi, B. *Angew. Makromol. Chem.* **1990**, 178, 209.
- (22) Borbély, J.; Katona, I.; Máth, Cs. *Magyar Kémiai Folyóirat (in Hungarian)* **1997**, 1, 22.
- (23) Stokr, J.; Schneider, B. *J. Appl. Polym. Sci.* **1979**, 23, 3553.

MA9908752